



## SODIUM ALGINATE FILM INCORPORATED WITH ZINC OXIDE NANOPARTICLES AS ANTIBACTERIAL AGENT

Bashar Alshami<sup>1</sup>, Wissam Zam<sup>2\*</sup> and Walid Khaddam<sup>1</sup>

<sup>1</sup>Department of Laboratory Diagnosis, Faculty of Pharmacy, Al-Baath University, Syria

<sup>2</sup>Department of Analytical and Food Chemistry, Faculty of Pharmacy, Tartous University, Syria

*Alginate biopolymer has been used in the design and development of several wound dressing materials such as (foams, topical formulations, nanofibers, films) due to its favorable properties, such as biocompatibility and non-toxicity. It has been particularly attractive in wound healing applications to date. Additionally, it can be loaded by antibacterial materials such as antibiotics, antibacterial plant extracts and metal nano-oxides. The aim of this study was to design sodium alginate (SA) based zinc oxide (ZnO) nanoparticles as antibacterial film for wound healing applications. The ZnO nanoparticles, with an average particle size of about 16.75 nm, were synthesized by sol-gel method and characterized by scanning electron microscope (SEM) and Fourier-transform infrared spectroscopy (FTIR). They were then incorporated as antibacterial into sodium alginate with different concentration (0, 5, 7.5, 10%). Effectiveness of antibacterial activity was carried out against Gram-negative bacteria (*Escherichia coli*, *Pseudomonas aeruginosa*) and Gram-positive bacteria (*Staphylococcus aureus*) to characterize the sample. The prepared ZnO/SA film presents a promising potential for applications as novel wound dressings*

**Keywords:** zinc oxide nanoparticles; sodium alginate; sol-gel method; antibacterial film; wound dressing

### INTRODUCTION

Zinc is a chemical element with an atomic number of 30 and an atomic weight of 65.73 (g/mol). It is a transitional element with a bright bluish-white color. It is the 23<sup>rd</sup> most abundant element in the earth's crust<sup>1</sup>. Zinc is found in many forms in nature, including zinc oxide, which appears in three crystal forms (Rock-salt, Zinc blende, Quartzite). Zinc oxide is used globally on a daily basis, and has been classified by The United States Food and Drug Administration (FDA) as a safe substance (GRAS). It has also been used as a food additive that increases the nutritional value of foods and helps improve appearance, flavor, and storage properties<sup>2&3</sup>. Zinc oxide is also used as an antibacterial, antifungal, and in many medical uses in particular, including: cosmetics and sunscreens as an emollient, skin moisturizer, and ultraviolet absorbent, in

addition to drug delivery, medical radiography, and biosensors<sup>4</sup>.

Nanoparticles are defined as particles whose dimensions range between (1-100) nm, that is, 10 to 9 times smaller than a meter. When these particles transform from their main size to the nano-size, they gain improved properties or completely new properties. Therefore, nanomaterials are considered useful factors in accelerating wounds healing process. This is because of its multiple advantages, such as high surface-to-volume ratio, as well as its ability to deliver drugs. These properties can improve collagen deposition and the remodeling of dermal tissue. The properties of nanoparticles allow them to penetrate well into wounds, which allows the manufacture of specific target particles to enter wounds and interact with it through biological interaction or secretion of drugs locally, which affects the progress of healing<sup>5</sup>. In addition, it is possible

to coat the drugs within the nanoparticles, and thus, they can be protected from proteases, allowing them to reach the target site without destroying them and achieving the required biological effect. That is, the biological nanoparticles are suitable for improving the wound healing process, which is due to the antibacterial properties in addition to the anti-inflammatory effectiveness and the ability to influence the extracellular matrix process (ECM) and stem cell proliferation and differentiation<sup>5</sup>. Zinc oxide nanoparticles are well known to exert antibacterial properties by disrupting bacterial cell wall via electrostatic interactions, generating reactive oxygen species that have a high lethal activity on bacteria via impacting the bacterial cell membrane, protein, DNA, and electron transport chain, and releasing Zn<sup>+2</sup> ions that induce an antimicrobial response in microorganisms due to interference in metabolic processes and disturbance in enzymatic systems<sup>6&7</sup>.

Alginates are considered biopolymers that are obtained from various sources of seaweed, especially in the outer wall of brown algae, which contain large quantities of them<sup>8</sup> and have many biomedical uses due to their properties such as biocompatibility, non-toxicity, moist environment, and their effectiveness in reducing bacterial infection, in addition to its effectiveness in stopping bleeding. These characteristics are among the important factors that must be available in a bandage. Therefore, alginate are used in medical bandages to this day, as it has been used and applied to medical gauze in different and varied forms such as (membranes - foams - films). The film form is the preferred one as it can be loaded with antibacterial materials, and improves the healing of wounds and burns, in addition to being permeable to water vapor, carbon dioxide and oxygen<sup>9</sup>.

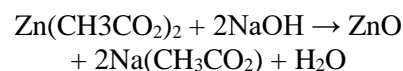
During this research, films of sodium alginate containing zinc nanoparticles will be prepared and applied to wounds and burns to help heal them.

## MATERIALS AND METHODS

### *Preparation of Zinc nanoparticles*

Zinc nanoparticles were prepared using (sol-gel) chemical method, so that zinc acetate dihydrate was used as a precursor compound,

ethanol as a reagent, and distilled water as a solution<sup>10</sup>, according to the following equation:



The preparation was done by weighing 10g of zinc acetate dihydrate, adding it to a beaker containing 75 \*ml of distilled water, and placed on the electric magnetic stirrer until complete dissolution for 15 min. After complete dissolution, 80% of sodium hydroxide solution was added to the zinc acetate solution at once with continuous stirring. Finally, absolute ethanol was added gradually (drop by drop) to the previous mixture until reaching pH= 10. After centrifugation, the precipitated white powder was collected in tubes and incinerated at 300° C for 1 hour where a white powder of zinc nanoparticles (ZnO-NPs) was obtained<sup>10</sup>.

The resulting powder was weighed and a weight of 7.36 g was obtained (**Fig. 1**), with a yield of 73.6%.



**Fig. 1:** yield of zinc oxide nanoparticles.

### *Characterization of nanoparticles*

1-FT-IR spectroscopy: The results of the chemical reaction were analyzed and confirmed by a FT-IR spectroscopy (SHIMADZU), where measurements were made between (400 and 4000 cm<sup>-1</sup>), so that the chemical bonds and functional groups were identified through absorption sites in the infrared spectrum.

2- Scanning Electron Microscopy SEM: A sample of the white powder was photographed by SEM with a maximum magnification of x500000 (Scanning Electron Microscopy Tescan VEGA) to confirm the formation of nanoparticles.

**Preparation of Sodium alginate film loaded with Zinc Nanoparticles**

The films (Fig. 2) were prepared with different concentrations of Zinc Oxide nanoparticles (0.5%, 7.5%, 10%) using sodium alginate at a concentration of 3% and glycerin as a plasticizer at a concentration of 10% as detailed in table 1. After that, 20 ml of the previous solutions were added to sterile gauze pieces sized (8×13) cm<sup>2</sup> and were left for 10 minutes until the gauze absorbed the whole solution. Finally, films were formed by ion gelation method using calcium chloride at a concentration of 5%. CaCl<sub>2</sub> solution was added to each film and left submerged for 5 min. Finally films were left to dry in were left to dry in an oven for 24 hrs at 40 °C.



**Fig. 2:** Sodium alginate film loaded with Zinc nanoparticles.

These films were applied to three types of microorganisms, namely:

- *Pseudomonas aeruginosa* ATCC 9027
- *Escherichia coli* ATCC 8739
- *Staphylococcus aureus* ATCC 6538

**Water vapor permeability**

In order to determine water vapor permeability (WVP), 5 g of anhydrous calcium chloride was added into Erlenmeyer flasks covered with different films and sealed using paraffin. These flasks were then placed in a desiccator containing water (100% relative humidity) at 25 °C. The weight of the Erlenmeyer flasks were for 12 hrs measured at 2 h intervals. Triplicate tests were taken.

The weight loss of the vials was recorded and plotted as a function of time. The water vapor Transmitted from the films (WVTR) was calculated from the slope of the straight line (g/s) divided by the cell area (m<sup>2</sup>).

Water vapor permeability was calculated using the following equation:

$$WVTR = Slope/A$$

$$WVP (g/m s Pa) = \frac{WVTR * D}{\Delta P}$$

Where A to the area (m<sup>2</sup>), D to the thickness of the film (m), and ΔP to the water vapor pressure differential between the two sides of the film (Pa).

**Table1:** The composition of different Sodium alginate film loaded with Zinc Nanoparticles

Sample number	Control film	Sample 1	Sample 2	Sample 3
ZnO-NPS (mg)	0	5	7.5	10
Distillated water (ml)	100	100	100	100
Sodium alginate (g)	3	3	3	3
Glycerol (ml)	10	10	10	10
Calcium Chloride 5% (ml)	50	50	50	50

## RESULTS AND DISCUSSION

### Results

#### Yield of nanoparticles

Starting from using zinc acetate dihydrate as a source of zinc in an amount of 10 grams, 7.36 grams of nanoparticles were finally obtained, with a percentage of 73.6%. This yield is close to the yield obtained by Venkataraju et al. (81.01%)<sup>11</sup> and Lopez-Cuenca et al. (85%)<sup>12</sup> during the preparation of nanoparticles by the chemical method. However, the yield obtained by the same researcher during the preparation of nanoparticles applying biological method by cold and hot extraction was much lower (24.66%, 24.30%) compared with the chemical method of preparation. Similar low yield was obtained by Wang et al. during the preparation of zinc nanoparticles by using coffee leaf extract<sup>13</sup>.

#### Infrared spectrum analysis

The following peak lengths were observed:

- Strongly extended belly-shaped crest between wavelength  $3200\text{ cm}^{-1}$  and  $3500\text{ cm}^{-1}$  indicating the O-H bond.
- An average absorption peak at  $1622\text{ cm}^{-1}$  indicating C=O bond.
- Superabsorbent peak at  $1413\text{ cm}^{-1}$  belonging to the C-O bond.

- A weak peak at  $990\text{ cm}^{-1}$  belonging to the C-C bond.
- A highly absorbent peak at  $418\text{ cm}^{-1}$  belonging to the Zn-O bond.
- The FT-IR peaks obtained in **Fig. (3)** were similar to those obtained by Keerthika et al.<sup>14</sup> who followed a similar method for synthesizing zinc nanoparticles. Additionally, similar FT-IR peaks were obtained by Shamhari et al.<sup>15</sup> who used the same synthesis method while using potassium hydroxide instead of sodium hydroxide as the precursor compound to perform the hydrolysis reaction.

However, the FT-IR peaks obtained by Kalpana et al.<sup>16</sup> were significantly different except for the main peak that belongs to zinc nanoparticles (ZnO) and this is maybe due to the use of a biosynthetic method for the preparation of nanoparticles based on *A. niger* fungus.

**Fig. (4)** showed the FT-IR peaks after purification and incineration. As noticed, the main peak of absorption  $418\text{ cm}^{-1}$  belonging to Zn-O bond was preserved, and this result was consistent with many previous researches<sup>17-19</sup> however was the method used the preparation of nanoparticles.

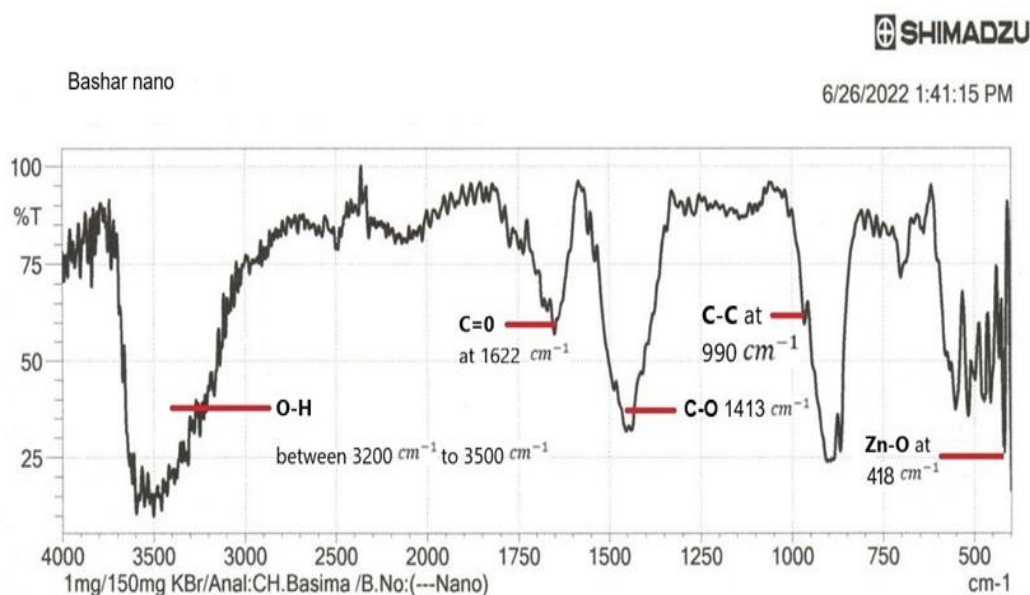


**Fig. 3:** FTIR spectrum of Zinc nanoparticles before purification and incineration.

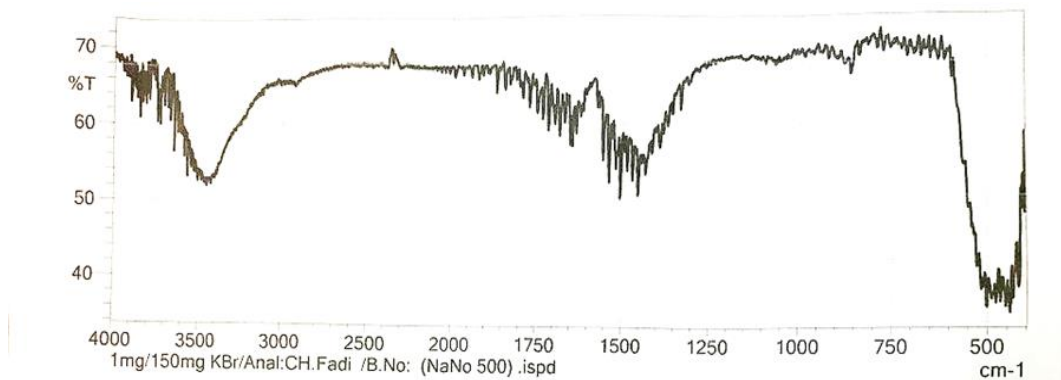


**Fig. 4:** FTIR spectrum of Zinc nanoparticles after purification and incineration.

**Scanning electron microscopy image analysis**

As shown in **Fig. (5)**, nanoparticles have a spherical shape. Their average dimension is 16.75 nm.

Our results are in accordance with the results of several previous studies<sup>14,20</sup> who followed the same method and parameters of preparation with only one exception, which is the use of methanol instead of ethanol as a reagent. The shapes of the particles were all spherical, and the dimensions of the particles ranged between 15 and 25 nanometers. This confirms that the detector had no effect on the shape of the nanoparticles.

As mentioned in previous researches, the shape and dimensions of the nanoparticles are related to several parameters during manufacturing process, including the reaction time, the incineration temperature, and the salt used and its concentration. Studies have shown that the formation of nanoparticles begins within minutes after adding the mineral salt, and their size increases as the reaction time increases<sup>21</sup>. This happens at three different stages and any increase in the timing leads to obtaining larger nanoparticles<sup>22&23</sup>. During incineration, the particles merge and increase in size, especially the crystal size<sup>24</sup>. A wide

number of studies showed the effect of incineration on the shape of the particles and its effect on the physical and chemical properties. Ashaf et al.<sup>25</sup> prepared zinc nanoparticles using sol-gel method and incineration at a temperature of 300 °C. The dimension of nanoparticles obtained ranged between 17-24 nm which is similar to the dimension of nanoparticles obtained in this research. However, incineration at a temperature of 500°C caused a significant increase of nanoparticles dimension (approximately 30 nm). Majumder et al.<sup>4</sup> explained the effect of using different salts as a source of zinc. When zinc chloride salt is used, the particles appeared in a hexagonal structure due to the the formation of an intermediate compound  $Zn_5(OH)_8Cl_2 \cdot H_2O$  which is fused with the nanocrystals to give the distinctive hexagonal shape. However, when zinc nitrate is used, two shapes were formed depending on the concentration of nitrates. At low concentrations of nitrates (1-3 M), the particles appear in the form of nano-sheets; however, when using a high concentration (5M), the particles aggregate more and appear in the form of nanorods<sup>26</sup>.

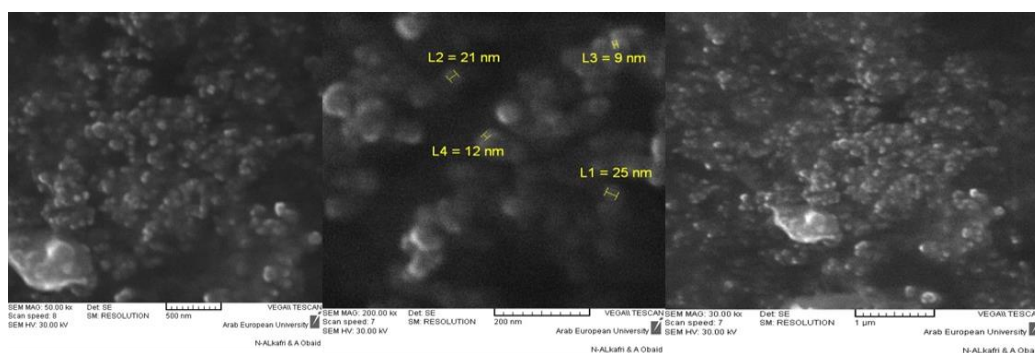


**Fig. 5:** A scanning electron microscope image of Zinc nanoparticles at several magnifications.

### Estimation of bacterial activity

As shown in **Fig. (6)**, zinc nanoparticles have antibacterial activity against Gram-negative and Gram-positive bacteria with a significant differences between different concentrations as confirmed by One way ANOVA test ( $p$ -value < 0.05), which is in agreement with many previous studies<sup>27&28</sup>. The antibacterial activity of Zinc nanoparticles is due by several mechanisms including the release of oxygen free radicals and the liberation of diploid Zinc ions.

As confirmed in many previous studies, the toxicity of free oxygen radicals to bacteria is due to their high activity and oxidative properties<sup>29&30</sup>. These free radicals could enter into the cell envelope and destroy cellular components such as lipids, DNA and proteins. Additionally, the antibacterial activity increases as the size of the nanoparticles decreases<sup>31</sup>.

Studies also showed that the release of free oxygen radicals happens on the surface of ZnO-Nps and suggested a link between photon interaction and antibacterial activity<sup>32</sup>.

The liberation of diploid Zinc ions is one of the main reasons for the antibacterial mechanism of Zinc nanoparticles<sup>33&34</sup> since the release of  $Zn^{2+}$  has a significant effect in inhibiting active transport and metabolism of amino acids in addition to disrupting the enzymatic system. There are many studies that confirmed that the leakage of Zinc ions with a double charge ( $Zn^{2+}$ ) in the bacterial growth medium is responsible for nanotoxicity and also found an inverse proportion between particle size and liberation of ions as free oxygen radicals.

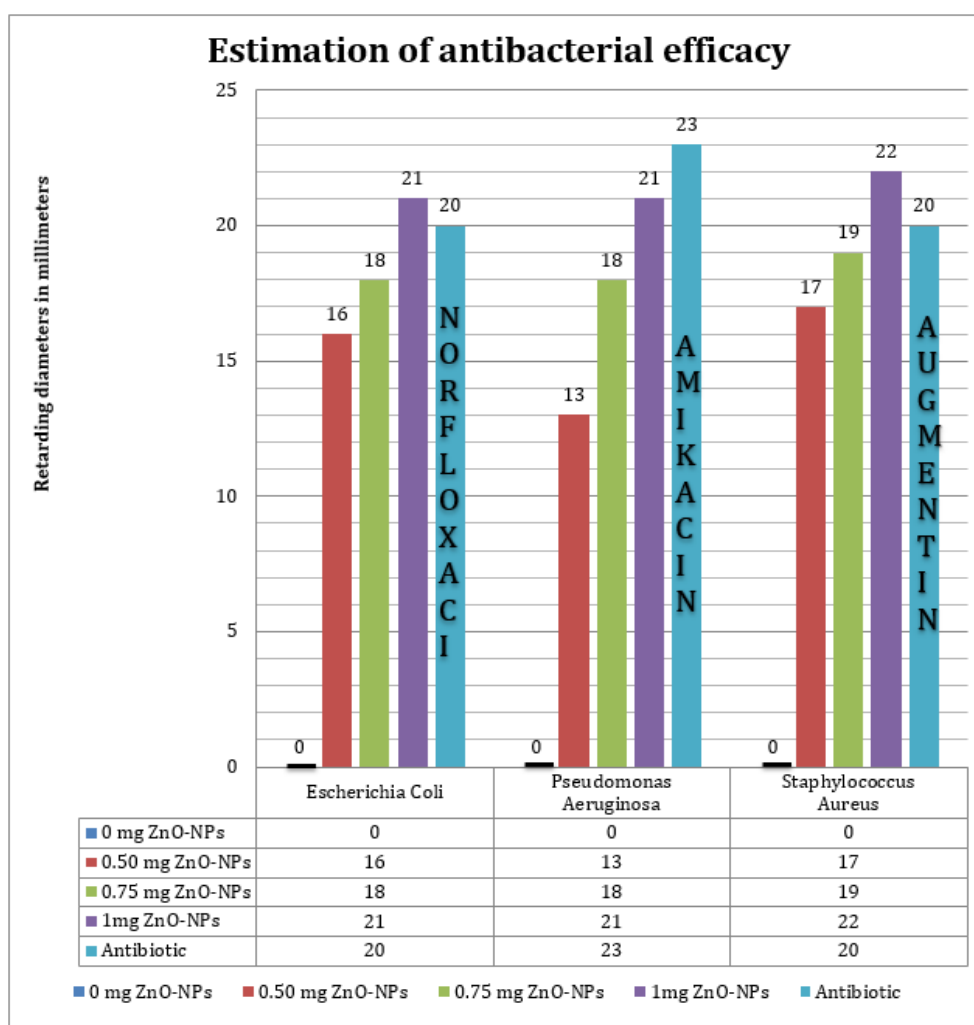


**Fig. 6:** Diameter of inhibition zone of ZnO nanoparticles at different concentration and typical antibiotic against gram-positive and gram-negative bacteria.

Pasquet et al.<sup>35</sup> concluded that the release of  $Zn^{2+}$  ions is related to two main reasons: the physicochemical properties of the particles and the chemistry of the reaction medium. Finally, Peng et al.<sup>36</sup> showed that particles with a spherical shape give more  $Zn^{2+}$  ions than particles with a rod shape.

Ismail et al.<sup>37</sup> also showed the significant effect of the incineration temperature on the antibacterial activity when preparing nanoparticles by the chemical sol-gel method. They prepared zinc nanoparticles with different degrees of incineration and studied their antibacterial activity and concluded that the best temperature that gave the highest antibacterial activity was 300°C which is consistent with this research and might be the reason for the strong antibacterial efficacy.

Naqvi et al.<sup>38</sup> explained the effect of particle dimensions and their role in the antibacterial effectiveness. The smaller the particle dimensions, the greater the ratio (surface area / volume), thus greater contact with germs. Additionally, the small dimension of nanoparticles was correlated with an increased secretion of double-charged zinc ions and reactive oxygen species which have a prominent role in antibacterial activity.

Finally, several researchers confirm<sup>39&40</sup> that the chemical method gave better antibacterial activity compared to the botanical method.

It is well known that the reduction of water vapor permeability can reduce economic losses and improve product quality and shelf life<sup>41</sup>. Generally, alginate films were reported to exhibit high water vapor permeability since they are hydrophilic films, but incorporation of calcium can significantly reduce the water vapor permeability<sup>42</sup>. The obtained values for WVP determination are presented in **Table 2**. WVP measurements showed a better performance for the films with higher ZnO NPs content as these particles act as a physical barrier impermeable to water and form a ZnO–alginate composite structure increasing the pathways for water molecules<sup>43</sup>.

**Table 2:** Water vapor permeability (WVP) for different alginate films.

Sample number	WVP ( $10^{-10}$ g/Pa.m.s)
1	4.627±0.025
2	4.126±0.012
3	3.628±0.018

## Conclusion

Medical gauze loaded with Sodium alginate film containing Zinc nanoparticles prepared in this study, showed clear activity against many types of gram-positive and gram-negative bacteria (*Pseudomonas aeruginosa*, *Escherichia coli*, *Staphylococcus aureus*), so it can be considered as a promising material in terms of the possibility of using it to accelerate the process of healing wounds and burns and maintaining their sterility, but this needs further studies related to stability and safety before applying it in-vivo to living tissues.

## REFERENCES

1. K. Kaur, R. Gupta, S. A. Saraf, and S. K. Saraf, "Zinc: the metal of life", *Compr Rev Food Sci Food Saf*, 13(4), 358-376 (2014).
2. A. Kołodziejczak-Radzimska and T. Jesionowski, "Zinc oxide—from synthesis to application: a review", *Materials*, 7(4), 2833-2881 (2014).
3. V. Parihar, M. Raja, and R. Paulose, "A brief review of structural, electrical and electrochemical properties of zinc oxide nanoparticles", *Rev Adv Mater Sci*, 53(2), 119-130 (2018).
4. S. Majumder, P. Basnet, J. Mukherjee, and S. Chatterjee, "Effect of zinc precursor on morphology of ZnO nanoparticles", *AIP Conf Proc*, 2273(1), 040006 (2020).
5. I. De Luca, P. Pedram, A. Moeini, P. Cerruti, G. Peluso, A. Di Salle, and N. Germann, "Nanotechnology development for formulating essential oils in wound dressing materials to promote the wound-healing process: A review" , *Appl Sci*, 11(4), 1713 (2021).
6. S.E. Jin and H.E. Jin, "Antimicrobial activity of zinc oxide nano/microparticles and their combinations against pathogenic microorganisms for biomedical applications: From physicochemical characteristics to pharmacological aspects", *Nanomaterials*, 11(2), 263 (2021).
7. E. Ren, C. Zhang, D. Li, X. Pang, and G. Liu, "Leveraging metal oxide nanoparticles for bacteria tracing and eradicating", *View*, 1(3), 20200052 (2020).

8. X. Gao, C. Guo, J. Hao, Z. Zhao, H. Long, and M. Li, "Adsorption of heavy metal ions by sodium alginate based adsorbent-a review and new perspectives", *Int J Biol Macromol*, 164, 4423-4434 (2020).
9. B.A. Aderibigbe and B. Buyana, "Alginate in wound dressings", *Pharmaceutics*, 10(2), 42 (2018).
10. J. Hasnidawani, H. Azlina, H. Norita, N. Bonnia, S. Ratim, and E. Ali, "Synthesis of ZnO nanostructures using sol-gel method", *Procedia Chemistry*, 19, 211-216 (2016).
11. J.L. Venkataraju, R. Sharath, M. Chandraprabha, E. Neelufar, A. Hazra, and M. Patra, "Synthesis, characterization and evaluation of antimicrobial activity of zinc oxide nanoparticles", *J Biochem Technol*, 3(5), 151-154 (2014).
12. S. López-Cuenca, L. P. Carrillo, M. R. Velasco, R. D. De León, H. Saade, R. López, E. Mendizábal, and J. Puig, "High-yield synthesis of zinc oxide nanoparticles from bicontinuous microemulsions", *J. Nanomater.*, 61-61 (2011).
13. Q. Wang, S. Mei, P. Manivel, H. Ma, and X. Chen, "Zinc oxide nanoparticles synthesized using coffee leaf extract assisted with ultrasound as nanocarriers for mangiferin", *Curr Res Nutr Food Sci*, 5, 868-877 (2022).
14. V. Keerthika, A. Ananth, and M. Rajan, "Synthesis, Characterization and Antibacterial Activity of Zinc Oxide Nanoparticles", *J Nanosci Nanotechnol*, 4(4), 439-442 (2018).
15. N.M. Shamhari, B.S. Wee, S.F. Chin, and K.Y. Kok, "Synthesis and characterization of zinc oxide nanoparticles with small particle size distribution", *Acta Chim Slov*, 2169(1), 060010 (2018).
16. V. Kalpana, B.A.S. Kataru, N. Sravani, T. Vigneshwari, A. Panneerselvam, and V.D. Rajeswari, "Biosynthesis of zinc oxide nanoparticles using culture filtrates of *Aspergillus niger*: Antimicrobial textiles and dye degradation studies", *Opennano*, 3, 48-55 (2018).
17. Y.A. Selim, M.A. Azb, I. Ragab, and M.H.M. Abd El-Azim, "Green synthesis of zinc oxide nanoparticles using aqueous extract of *Deverra tortuosa* and their cytotoxic activities", *Sci Rep*, 10(1), 3445 (2020).
18. T. Varadavenkatesan, E. Lyubchik, S. Pai, A. Pugazhendhi, R. Vinayagam, and R. Selvaraj, "Photocatalytic degradation of Rhodamine B by zinc oxide nanoparticles synthesized using the leaf extract of *Cyanometra ramiflora*", *J Photochem Photobiol B, Biol*, 199, 111621 (2019).
19. M.H. Kahsay, "Synthesis and characterization of ZnO nanoparticles using aqueous extract of *Becium grandiflorum* for antimicrobial activity and adsorption of methylene blue", *Water Sci Eng*, 11(2), 45 (2021).
20. G. Singh and S.P. Singh, "Synthesis of zinc oxide by sol-gel method and to study its structural properties", *AIP Conf Proc*, 2220(1), 020184 (2020).
21. K. Chitra and G. Annadurai, "Antibacterial activity of pH-dependent biosynthesized silver nanoparticles against clinical pathogen", *BioMed Res Int*, 2014, 6 (2014).
22. U. Manzoor, F.T. Zahra, S. Rafique, M.T. Moin, and M. Mujahid, "Effect of synthesis temperature, nucleation time, and postsynthesis heat treatment of ZnO nanoparticles and its sensing properties", *J Nanomater*, 16(1), 189058 (2015).
23. I.S. Smolkova, N.E. Kazantseva, V. Babayan, J. Vilcakova, N. Pizurova, and P. Saha, "The role of diffusion-controlled growth in the formation of uniform iron oxide nanoparticles with a link to magnetic hyperthermia", *Cryst Growth Des*, 17(5), 2323-2332 (2017).
24. A.J. Ruys, *Alumina ceramics: biomedical and clinical applications*. Woodhead Publishing, Duxford, United Kingdom, 2019, p.558.
25. R. Ashraf, S. Riaz, Z.N. Kayani, and S. Naseem, "Effect of Calcination on properties of ZnO nanoparticles", *Mater Today: Proc*, 2(10), 5468-5472 (2015).
26. R. Singh and S. Dutta, "The role of pH and nitrate concentration in the wet chemical growth of nano-rods shaped ZnO photocatalyst", *Nano-Struct Nano-Objects*, 18, 100250 (2019).
27. K. S. Siddiqi and A. Husen, "Properties of zinc oxide nanoparticles and their activity

- against microbes", *Nanoscale Res Lett*, 13(1), 1-13 (2018).
28. B. Lallo da Silva, M.P. Abuçafy, E. Berbel Manaia, J.A. Oshiro Junior, B.G. Chiari-Andréo, R.C.R. Pietro, and L.A. Chiavacci, "Relationship between structure and antimicrobial activity of zinc oxide nanoparticles: An overview", *Int J Nanomedicine*, 14, 9395-9410 (2019).
  29. A. Sirelkhatim, S. Mahmud, A. Seeni, N.H.M. Kaus, L.C. Ann, S.K.M. Bakhori, H. Hasan, and D. Mohamad, "Review on zinc oxide nanoparticles: antibacterial activity and toxicity mechanism", *Nanomicro Lett*, 7, 219-242 (2015).
  30. M.G. Demissie, F.K. Sabir, G.D. Edossa, and B.A. Gonfa, "Synthesis of zinc oxide nanoparticles using leaf extract of lippia adoensis (koseret) and evaluation of its antibacterial activity", *J Chem*, 2020, 1-9 (2020).
  31. N. Padmavathy and R. Vijayaraghavan, "Enhanced bioactivity of ZnO nanoparticles—an antimicrobial study", *Sci Technol Adv Mater*, 9(3), 035004 (2008).
  32. Y. Xie, Y. He, P. L. Irwin, T. Jin, and X. Shi, "Antibacterial activity and mechanism of action of zinc oxide nanoparticles against *Campylobacter jejuni*", *Appl Environ Microbiol*, 77(7), 2325-2331 (2011).
  33. M. Premanathan, K. Karthikeyan, K. Jeyasubramanian, and G. Manivannan, "Selective toxicity of ZnO nanoparticles toward Gram-positive bacteria and cancer cells by apoptosis through lipid peroxidation", *Nanomed: Nanotechnol Biol Med*, 7(2), 184-192 (2011).
  34. M. Li, L. Zhu, and D. Lin, "Toxicity of ZnO nanoparticles to *Escherichia coli*: mechanism and the influence of medium components", *Environ Sci Technol*, 45(5), 1977-1983 (2011).
  35. J. Pasquet, Y. Chevalier, E. Couval, D. Bouvier, G. Noizet, C. Morlière, and M.-A. Bolzinger, "Antimicrobial activity of zinc oxide particles on five microorganisms of the Challenge Tests related to their physicochemical properties", *Int J Pharm*, 460(1-2), 92-100 (2014).
  36. X. Peng, S. Palma, N.S. Fisher, and S. S. Wong, "Effect of morphology of ZnO nanostructures on their toxicity to marine algae", *Aquat. Toxicol.*, 102(3-4), 186-196 (2011).
  37. A. Ismail, A. Menazea, H.A. Kabary, A. El-Sherbiny, and A. Samy, "The influence of calcination temperature on structural and antimicrobial characteristics of zinc oxide nanoparticles synthesized by Sol-Gel method", *J Mol Struct*, 1196, 332-337 (2019).
  38. Q.A. Naqvi, A. Kanwal, S. Qaseem, M. Naeem, S.R. Ali, M. Shaffique, and M. Maqbool, "Size-dependent inhibition of bacterial growth by chemically engineered spherical ZnO nanoparticles", *J Biol Phys*, 45, 147-159 (2019).
  39. H.M. Abdelmigid, N.A. Hussien, A.A. Alyamani, M.M. Morsi, N.M. AlSufyani, and H.A. Kadi, "Green synthesis of zinc oxide nanoparticles using pomegranate fruit peel and solid coffee grounds vs. chemical method of synthesis, with their biocompatibility and antibacterial properties investigation", *Molecules*, 27(4), 1236 (2022).
  40. K.R. Ahammed, M. Ashaduzzaman, S.C. Paul, M.R. Nath, S. Bhowmik, O. Saha, M.M. Rahaman, S. Bhowmik, and T.D. Aka, "Microwave assisted synthesis of zinc oxide (ZnO) nanoparticles in a noble approach: utilization for antibacterial and photocatalytic activity", *SN Appl Sci*, 2, 1-14 (2020).
  41. A. Kurt, O.S. Toker and F. Tornuk, "Effect of xanthan and locust bean gum synergistic interaction on characteristics of biodegradable edible film", *Int J Biol Macromol*, 102, 1035-1044 (2017).
  42. T. Senturk Parreidt, K. Muller and M. Schmid, "Alginate-based edible films and coatings for food packaging applications", *Foods*, 7(10), 170 (2018).
  43. A. Valdes, E. Garcia-Serna, A. Martinez-Abad, F. Vilaplana, A. Jimenez and M.C. Garrigos, "Gelatin-based antimicrobial films incorporating pomegranate (*Punica granatum L.*) seed juice by-product", *Molecules*, 25(1), 166 (2020).



## نشرة العلوم الصيدلانية جامعة أسيوط



### القدرة المضادة للجراثيم لأفلام الجينات الصوديوم المحملة بأكسيد الزنك النانوي

بشار الشامي<sup>١</sup> - وسام زم<sup>٢\*</sup> - وليد خدام<sup>١</sup>

<sup>١</sup> قسم التشخيص المخبري، كلية الصيدلة، جامعة البعث، سوريا

<sup>٢</sup> قسم الكيمياء التحليلية والغذائية، كلية الصيدلة، جامعة طرطوس

استعملت الجينات الصوديوم من أجل تطوير العديد من مواد تضميد الجروح (الغرويات، المركبات الموضعية، الألياف النانوية، الأفلام) نظراً لتوافقه الحيوي وأمانه. كما يمكن تحميل بعض المواد المضادة للبكتيريا على الجينات الصوديوم مثل الصادات الحيوية والخلاصات النباتية وأكاسيد المعادن النانوية. تهدف هذه الدراسة إلى تطوير فيلم من الجينات الصوديوم محمل بأكسيد الزنك النانوي كضاد مضاد للبكتيريا يساعد على التئام الجروح. تم تحضير أكسيد الزنك النانوي بأبعاد ١٦,٧٥ نم وذلك باتباع الطريقة الكيميائية في التصنيع. فحصت الجسيمات النانوية المحضرة باستعمال المجهر الإلكتروني وطيف الأشعة تحت الحمراء. ومن ثم تم تحميل أفلام الجينات الصوديوم بالجسيمات النانوية المحضرة بتركيز مختلفة (٠، ٥، ٧,٥، ١٠ %). تم تحديد الفعالية المضادة للبكتيريا على بعض البكتيريا سلبية الغرام (*Escherichia coli*, *Pseudomonas aeruginosa*) وبعض البكتيريا إيجابية الغرام (*Staphylococcus aureus*). بينت النتائج أن الأفلام المحضرة تمثل طريقة مستقبلية واعدة للمساعدة في التئام الجروح من خلال فعاليتها المضادة للبكتيريا.